Feasibility and Synthesis of Hybrid Reactive Distillation Systems

Nitin Chadda and Michael F. Malone
Dept. of Chemical Engineering, University of Massachusetts, Amherst, MA 01003

Michael F. Doherty
Dept. of Chemical Engineering, University of California, Santa Barbara, CA 93106

A systematic method to synthesize hybrid reactive distillation configurations described here uses three building blocks. These building blocks are a cocurrent rectifying cascade, a cocurrent stripping cascade, and a countercurrent cascade. A feasibility diagram and a product purity diagram provide a global view of the "direct" and "indirect" sharp split products that can be obtained as a function of the reaction rate from single−feed and double−feed hybrid columns, respectively. These diagrams are used as a basis for quickly and systematically generating feasible column configurations (if any) that produce the desired product. Three esterification examples are used to illustrate the method. In spite of the fact that the examples form a homologous series, the feasible designs are quite different. The results compare well with column simulations.

Introduction

A conventional chemical process frequently includes a reactor followed by a separation system, often distillation. In reactive distillation, the two processes are combined so that synergistic effects between reaction and separation can occur. The advantages of combining reaction with distillation were recognized long ago (Backhaus, 1921; Keyes, 1932; Longtin and Randall, 1942), but the idea did not capture the imagination of people in the process industry until much later (Agreda and Partin, 1984). Because of the potential advantages of this technology (capital productivity and selectivity improvements, reduced energy use, and reduction or elimination of solvents), several techniques for designing reactive distillation columns have been proposed in the past decade. The methods include:

(a) Geometric/fixed point methods (Barbosa and Doherty, 1988a,b; Buzad and Doherty, 1994; Okasinski and Doherty, 1998; Melles et al., 2000)

(b) Difference point methods (Hauan et al., 2000; Lee et al., 2000a,b)

(c) Mixed integer nonlinear programming methods (Ciric and Gu, 1994; Papalexandri and Pistikopoulos, 1996; Ismail et al., 1999)

(d) Simulated annealing methods (Cardoso et al., 2000).

All of these methods require the specification of feasible products, without which the design process can be difficult, if not impossible. Thus, a feasibility analysis is important to find the regions of the composition space that are accessible via reaction and separation.

Estimation of feasible distillates and bottoms compositions for staged reactive distillation columns can be divided into three cases on the basis of the rate of reaction: extremely slow rates (no reaction limit); intermediate rates (kinetic regime); and very fast reaction rates (chemical equilibrium limit). In the limits of no reaction and of chemical equilibrium, various methods can be used to address feasibility (Wahnshafft et al., 1992; Fidkowski et al., 1993; Rooks et al. 1998; Ung and Doherty, 1995a,b; Espinosa et al., 1995; Bessling et al., 1997).

Feasibility studies at finite rates of reaction are interesting, because most reactive distillation devices operate in this regime. Giessler et al. (1998, 1999) use "static analysis" to determine feasibility of reactive columns operated with large internal flows. Chadda et al. (2000) described an algorithm to calculate the feasible product regions for a single−feed, staged continuous column in the kinetic regime using pinch tracking methods and the design equations for the rectifying and

Correspondence concerning this article should be addressed to M. F. Malone.

stripping sections. However, that method is practically limited to ternary systems.

Chadda (2001) and Chadda et al. (2001) describe a simpler and more generally applicable model for flash cascades to address the issue of feasibility in single−feed, fully reactive, continuous columns. A bifurcation study provides a global view of the "direct" and "indirect" sharp splits at all rates of reaction. (One of the products in a sharp split will be either a pure component, an azeotrope, or a kinetic pinch point.) The main advantages of the flash cascade model are:

(a) It provides a global view of feasibility as a function of the production rate, catalyst concentration, and liquid holdup.

(b) It applies to any number of components and reactions.

(c) It can be implemented and interpreted quickly.

At present, few methods are available to assess the feasibility of hybrid and double−feed columns for finite rates of reaction. The purpose of this article is to develop a flash cascade model for hybrid columns and double−feed reactive distillation columns. The methods used in this article can be used to answer the following questions at the conceptual design stage.

(a) What ranges (if any) of production rates, catalyst concentrations, and liquid holdups are suitable to obtain the desired product?

(b) What kind of column configuration (if any) is suitable to get the desired product, viz, a single−feed or a double−feed column; reactive or hybrid column?

(c) For each feasible column configuration that exists, what are the composition of the two products comprising the split?

Feasibility of Single−feed Columns

Fully reactive columns

Chadda et al. (2001) provide a model based on cocurrent cascades of isobaric flash reactors (Figure 1) to determine the feasibility of fully reactive continuous columns. The rectifying and stripping cascades in Figure 1 are surrogates for the rectifying and stripping sections in a continuous column, respectively.

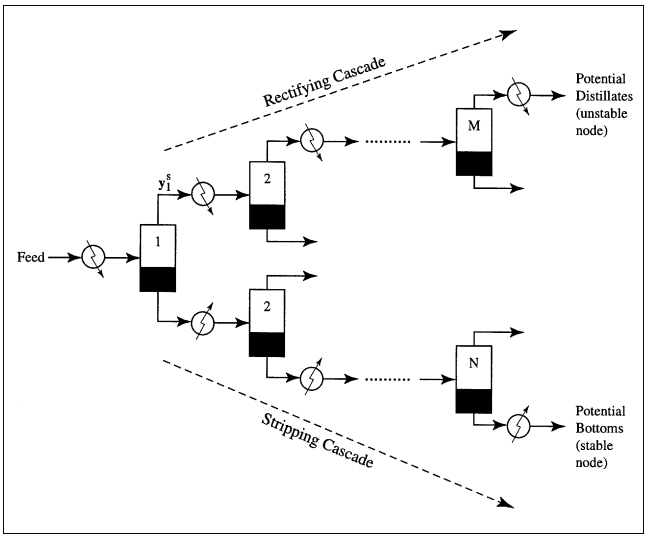

Figure 1. Single-feed fully reactive flash cascades.

The model for the stripping cascade of N stages is

$$x_{i,j-1} = \phi y_{i,j} + (1-\phi)x_{i,j} - \nu_i\left(\frac{k_f}{k_{f,\mathrm{ref}}}\right)\left(\frac{D}{1-D}\right)r(\boldsymbol{x}_j)$$

$$(i = 1.....c-1)$$

$$(j = 1,2.....N) \quad (1)$$

where $\boldsymbol{x}_0 = \boldsymbol{x}_F$. For the rectifying cascade of M stages

$$y_{i,j-1} = \phi y_{i,j} + (1-\phi)x_{i,j} - \nu_i\left(\frac{k_f}{k_{f,\mathrm{ref}}}\right)\left(\frac{D}{1-D}\right)r(\boldsymbol{x}_j)$$

$$(i = 1.....c-1)$$

$$(j = 2,3.....M) \quad (2)$$

where $\boldsymbol{y}_1 = \boldsymbol{y}_1^s$, and $\boldsymbol{y}_1^s$ is the vapor stream composition from the first flash device of the stripping cascade shown in Figure 1. For definitions of the terms and for model development, see Chadda et al. (2001).

The two independent parameters for each flash unit are ϕ and D. ϕ is the fraction of feed vaporized in the unit and D is a normalized Damköhler number (Da, Damkohler, 1939) defined as $D = Da/(1+Da)$. Da is a function of the production rate, liquid holdup and catalyst concentration and is defined as in Chadda et al. (2001). No reaction occurs in the limit of $D_a \to 0$ ($D \to 0$) and reaction equilibrium is achieved as $Da \to \infty$ ($D \to 1$). At intermediate Da, the cascade operates in the kinetically controlled regime.

For the sharp split products from a continuous column, the fixed point branches of interest are the stable node branches in the stripping cascade and unstable node branches in the rectifying cascade; these are a function of D. These solution branches when plotted together comprise the *feasibility diagram* for a single−feed column. The feasibility diagram provides a global view of the products expected from a continuous distillation at *any* rate of reaction (or D). Chadda et al. (2001) provide a rule for feasibility as follows.

Rule for Feasibility: *Unstable node branches in the feasibility diagram represent potential distillates while the stable node branches represent the potential bottoms from a continuous single−feed reactive column.*

These fixed points $\hat{\boldsymbol{x}}$ for the stripping cascade (Eq. 1) are solutions of

$$(1-D)(\hat{x}_i - \hat{y}_i) + \nu_i\left(\frac{k_f}{k_{f,\mathrm{ref}}}\right)\left(\frac{D}{\phi}\right)r(\hat{\boldsymbol{x}}) = 0$$

$$(i = 1.....c-1) \quad (3)$$

where $\hat{\boldsymbol{x}}$ and $\hat{\boldsymbol{y}}$ are in vapor liquid equilibrium with each other. Similarly, the fixed points $\hat{\boldsymbol{y}}$ for the rectifying cascade (Eq. 2)

Table 1. Vapor Pressure Data for the Butyl Acetate System

Component	A_1	A_2	A_3	A_4	A_5
Acetic acid(1)	15.1923	−3,654.62	−45.392	0	0
n-Butanol(2)	108.826	−10,069.5	0	−13.256	4.38×10^{-6}
n-Butyl acetate(3)	103.79	−8,763.56	0	−13.118	8.439×10^{-6}
Water(4)	16.3178	−3,835.18	−45.343	0	0

Extended Antoine's equation:

$$\ln(P^{sat}) = A_1 + \frac{A_2}{(A_3+T)} + A_4 \ln(T) + A_5 T^2$$

P^{sat} [kPa]; T [K]

are solutions of

$$(1-D)(\hat{x}_i - \hat{y}_i) - \nu_i \left(\frac{k_f}{k_{f,\mathrm{ref}}}\right)\left(\frac{D}{1-\phi}\right) r(\hat{x}) = 0 \qquad (i = 1 \ldots\ldots c-1) \quad (4)$$

where $\hat{x}$ and $\hat{y}$ are in vapor liquid equilibrium with each other.

Consider the esterification of acetic acid with *n*-butanol at 1 atm

$$n-\mathrm{Butanol(BuOH)} + \mathrm{AceticAcid(HOAc)} \Leftrightarrow n-\mathrm{ButylAcetate(BuOAc)} + (\mathrm{Water}(H_2O)) \quad (5)$$

We represent the kinetics by a pseudo homogeneous model

$$r = k_f \left(a_{\mathrm{HOAc}} a_{\mathrm{BuOH}} - \frac{a_{\mathrm{BuOAc}} a_{H_2O}}{K_{\mathrm{eq}}}\right) \qquad (6)$$

where k_f is the forward rate constant. This is assumed constant over the temperature range of interest, along with the reaction equilibrium constant, which has a value of approximately 12.5 (Venimadhavan et al., 1999a). The vapor–liquid equilibrium was modeled with the Wilson equation and the vapor phase was taken as ideal, except for dimerization of acetic acid. The physical property data are provided in Tables 1 and 2.

The feasibility diagram at $\phi = 0.5$ is shown in Figure 2. The feasible distillate branch begins at the BuOAc–water azeotrope for $D = 0$ and ends in a quaternary reactive azeotrope at the chemical equilibrium limit, $D = 1$. The feasible bottoms products are: a BuOAc branch that is a solution for the entire range of D; a branch starting from BuOH–HOAc azeotrope that ends in a quaternary fixed point at $D = 0.03$; and a BuOH branch for $0.35 < D \le 1.0$. Three different feasibility structures are obtained from the diagram:

(a) For $0 < D < 0.03$, the potential distillates are quaternary mixtures and the potential bottoms are either BuOAc or quaternary mixtures, depending on the feed and the column design

(b) For $0.03 < D < 0.35$, the potential distillates are quaternary mixtures and the only feasible bottoms product is BuOAc

(c) For $0.35 < D < 1.0$, the potential distillates are quaternary mixtures and the potential bottoms are BuOAc or BuOH, depending on the feed and the column design.

Thus, BuOAc can be obtained as bottoms product from a single–feed fully reactive column at any rate of reaction, provided that the feed composition is in the appropriate range. The optimum design depends on a tradeoff between the liquid holdup and the number of stages in the column. For lower D, BuOAc may be produced with less holdup on each stage, but may require a large number of stages. At large D, BuOAc may be produced with large holdup on each stage, but with a lower number of stages.

Table 2. Binary Interaction Parameters for Wilson's Equation for Butyl Acetate System

$a_{11} = 0.0$	$a_{21} = 473.342$	$a_{31} = 674.184$	$a_{41} = 537.512$
$a_{12} = -162.658$	$a_{22} = 0.0$	$a_{32} = 149.858$	$a_{42} = 616.69$
$a_{13} = 1{,}231.476$	$a_{23} = 530.0937$	$a_{33} = 0.0$	$a_{43} = 2{,}199.218$
$a_{14} = 229.098$	$a_{24} = 26{,}314.2$	$a_{34} = 26{,}314.3$	$a_{44} = 0.0$

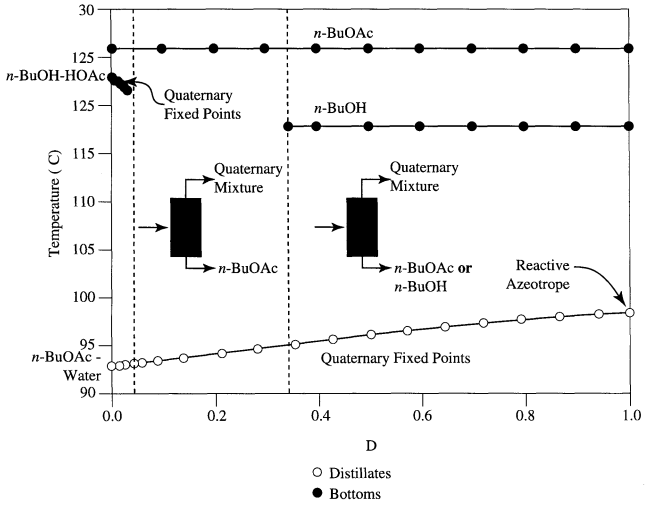

Figure 2. Feasibility diagram for butyl acetate system at 1 atm.

Hybrid columns

Combining reactive and nonreactive sections in a single column is essential in order to achieve certain products, depending on the mixtures and chemistries involved. For example, nonreactive barriers (such as azeotropes and distillation boundaries) may be overcome in reactive sections while reactive barriers (such as reactive azeotropes or kinetic pinch points) may be overcome in nonreactive sections. This can lead to higher conversions and/or higher selectivities. We are interested in finding feasible splits for hybrid columns which combine both reactive and nonreactive sections.

A method for assessing feasibility in hybrid columns is based on the hybrid flash cascade model shown in Figure 3. This represents a single–feed continuous column with a reactive middle section and nonreactive rectifying and stripping sections. We can construct different hybrid column configurations by mixing and matching the reactive and nonreactive flash cascades.

Figure 4 shows the hybrid feasibility diagram for the BuOAc system. For a fully reactive column (a) operated at $D = 0.6$

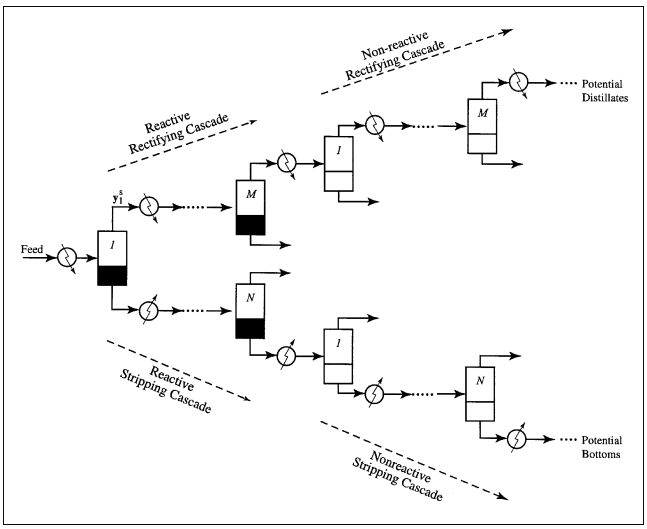

Figure 3. Single-feed hybrid flash cascades corresponding to Figure 4c.

(say), the potential distillate will be a quaternary mixture (point 2) and the bottoms will be either BuOAc or BuOH depending on the feed composition. Since BuOAc is the desired product, we choose it to be the potential bottoms composition (point 3).

If we add a nonreactive section on top of the reactive section, we generate a hybrid column configuration (b). This is equivalent to a hybrid flash cascade arrangement with a reactive rectifying cascade followed by a nonreactive rectifying cascade. The bottom half of the cascade contains a reactive stripping cascade. Starting from the feed composition, the reactive rectifying and stripping cascades can potentially lead to pinch points 2 and 3, respectively, at $D = 0.6$. Pinch point 2 is the feed to the nonreactive rectifying cascade; the trajectory of this cascade will head towards the "lightest boiling species" at $D = 0$ which is the butyl acetate–water azeotrope

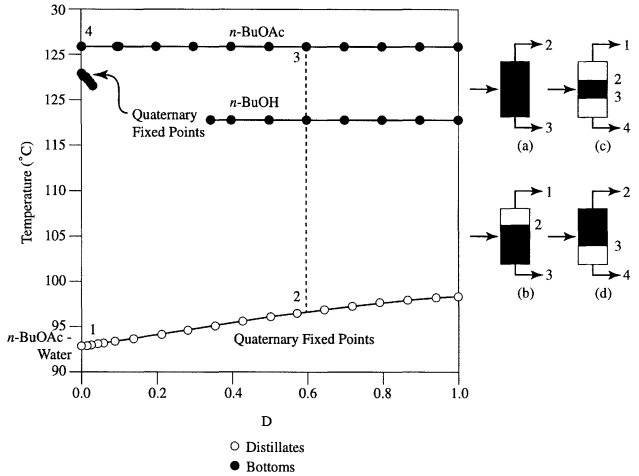

Figure 4. Feasibility diagram for butyl acetate showing products from different column configurations.

(point 1). Thus, introducing a nonreactive section leads to higher conversion and easier downstream processing because the distillate is a binary mixture (as opposed to a quaternary mixture from a fully reactive column).

If we introduce a nonreactive stripping section to configuration (b), hybrid column configuration (c) is generated whose flash cascade equivalent is shown in Figure 3. Adding a nonreactive stripping section does not change the potential bottoms (BuOAc), because it is also the "heaviest boiling species" at $D = 0$ (point 4). Apart from having the advantages attributed to configuration (b), configuration (c) is useful from an operational perspective because the nonreactive stripping section provides a safeguard against the loss of catalytic activity in the reactive section. Therefore, the column can be operated for a longer time than configuration (b) before the catalyst is replaced. Configuration (d) can be interpreted likewise with the feasibility diagram. The products from configuration (d) are a quaternary mixture as distillate and BuOAc as the bottoms.

Any of the four column configurations shown in Figure 4 are feasible process alternatives for producing high purity butyl acetate. However, configuration (c) seems more desirable than the others because of higher conversion, easier downstream processing, and operational reasons mentioned above.

For each chosen column configuration, we need to estimate the compositions of products in overall mass balance with each other. We consider configuration 4c. The potential products from this hybrid configuration are BuOAc–water azeotrope as a distillate and BuOAc as a bottoms. However, whether or not the two products can be obtained simultaneously depends on their satisfying the overall mass balance. To check for that, we solve the flash cascades equivalent of configuration 4c, which is shown in Figure 3.

The flash cascade trajectories (solutions of Eqs. 1 and 2 for a c component system are described with $(c-1)$ mole fractions. For chemical equilibrium limited reactions, it is more convenient to use the variable transformations introduced by Barbosa and Doherty (1988a,b) for single reactions and later extended by Ung and Doherty (1995a,b) to any number of reactions (R). These are also useful in kinetically–controlled circumstances. Here, we use these to project the trajectories in mole–fraction space onto a lower dimensional *reaction invariant* space with dimensionality $(c - R - 1)$. The advantage of the reaction invariants is that the lever rule mass balance is satisfied in these variables for equilibrium–limited reactive distillation.

These transforms are not complete for kinetically controlled reactions. We use a set of "composite variables" for expressing the solutions of cascades operated in the kinetically controlled regime; these are the $(c - R - 1)$ reaction invariants and R mole fraction variables. The R mole fractions are taken as the reference variables used to calculate the reaction invariants and are chosen in accordance with the rules given in Ung and Doherty (1995a). The reaction invariants are (Ung and Doherty)

$$X_i = \frac{x_i \nu_k - x_k \nu_i}{\nu_k - \nu_T x_k} \tag{7}$$

where $k = 1, \ldots, R$ are the reference components and $i = 1, \ldots, c - R - 1$.

The resulting composite variable space is $c - 1$ dimensional and each point on the cascade trajectory in this composite space has a one–to–one correspondence with the cascade trajectory in the $(c - 1)$ dimensional mole fraction space. An advantage of expressing solutions in the composite variable space is also in the ease of visualization of trajectories.

For example, in the BuOAc system, there are four components and a single reaction. Therefore, the composite variable space is three-dimensional (3-D) with two reaction invariants and one mole fraction variable. The mole fraction variable is the reference variable and is chosen here as x_{BuOAc}. The two transformed variables are then calculated using Eq. 7

$$X_1 = x_{\mathrm{HOAc}} + x_{\mathrm{BuOAc}}$$
$$X_2 = x_{\mathrm{BuOH}} + x_{\mathrm{BuOAc}} \tag{8}$$

Thus, X_1, X_2 and x_{BuOAc} comprise the composite variables set and the resulting solution space is the tetrahedral space within the "cube" shown in Figure 5a. Each vertex of the tetrahedron represents a pure component. The reaction invariants X_1 and X_2 can also be interpreted here as the fraction of acetate groups (Ac) and the fraction of butyl groups (Bu) in the mixture. These do not change on account of reaction, but only due to to vaporization.

Next, we solve the flash cascade equivalent for the hybrid column configuration shown in Figure 4c. The feed to the cascade is an equimolar mixture of acetic acid and butanol. Starting from the feed composition, Eq. 1 is solved recursively at $D = 0.6$ and $\phi = 0.5$ for a large number of stages until a point is reached where the composition is essentially constant from stage to stage. This pinch point is butyl acetate. The composition of the pinch point is taken as the feed to a nonreactive stripping cascade (Eq. 1 at $D = 0$). The corresponding pinch point from the nonreactive cascade is butyl acetate as expected. The mole fraction iterates from the stripping cascades are converted to composite variables using Eq. 8 with the results shown in Figure 5a. In a similar fashion, the rectifying cascade model (Eq. 2 at $D = 0.6$) is solved recursively for a large number of stages until a pinch point (quaternary mixture) is reached; this quaternary mixture is then taken as feed to a nonreactive rectifying cascade (Eq. 2 at $D = 0$). The corresponding pinch point from the nonreactive cascade is the butyl acetate–water azeotrope. The vapor mole fractions from the rectifying cascade trajectory are shown in Figure 5a.

To satisfy the overall mass balance, we make the orthogonal projection of the hybrid flash cascade trajectories in Figure 5a onto the base of the cube which is the reaction invariant space. The result is shown in Figure 5b. Each vertex of the transformed space is a pure component and each edge represents a nonreactive binary mixture. The desired product (BuOAc) is the potential bottoms. Next, we apply the lever rule for a continuous column by which the distillate, feed, and bottoms compositions lie on a straight line in a transformed variable space, as shown in Figure 5b. The point of intersection of the mass balance line and the stripping cascade trajectory (Butyl acetate–water azeotrope) indicates a feasible split.

The resulting estimate for a feasible split is shown in Table 3. To verify that such a split is obtained from a column, we also did column simulations using the same physical property models and kinetics. The column configuration chosen had a middle reactive section, with $D = 0.6$ for all reactive stages and, nonreactive rectifying and stripping sections. Starting with an initial estimate for the number of stages from the cascade calculation and the ratio of the product flows from

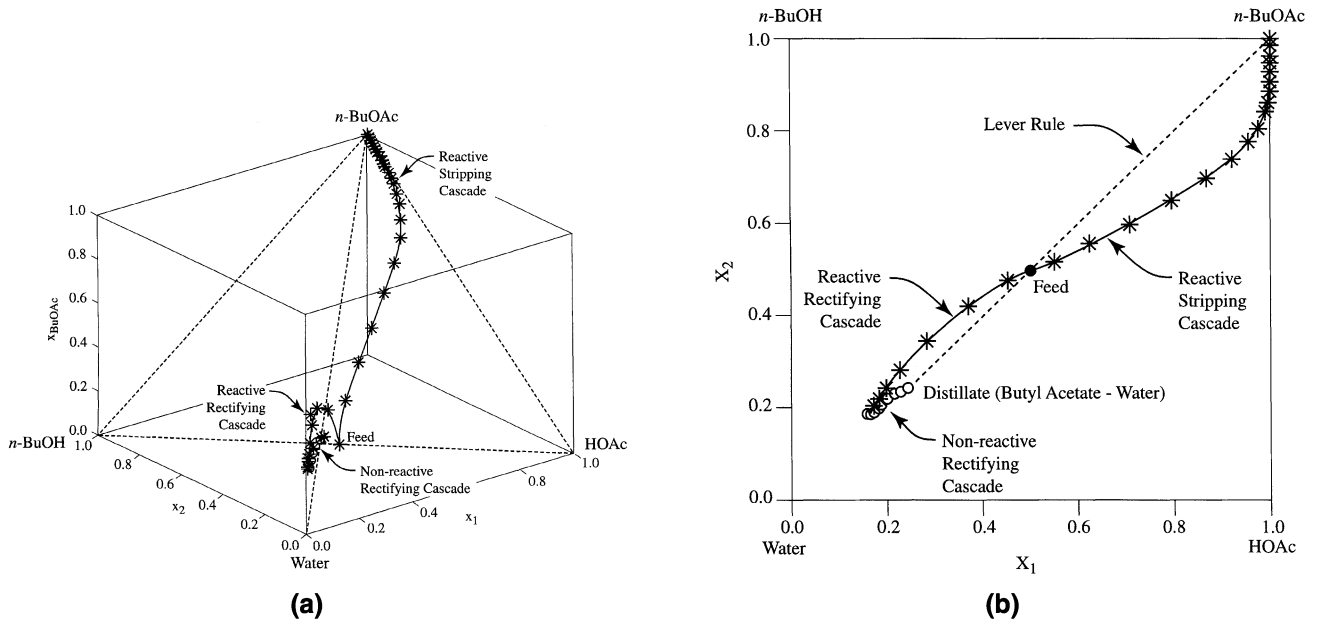

Figure 5. Flash cascade trajectories for a single-feed hybrid column for butyl acetate system in: (a) composite variable space; (b) reaction invariant space.

Table 3. Feasible Splits for Butyl Acetate System Predicted by the Hybrid Flash Cascade Model vs. Column Simulations at $D = 0.6$ for Splits in Figures 5 and 6

Mole Fraction	Cascade Prediction	Column Simulation*
Distillate		
HOAc	0.0	0.0
BuOH	0.0	0.0
BuOAc	0.247	0.235
Water	0.753	0.745
Bottoms		
HOAc	0.0	0.008
BuOH	0.0	0.0
BuOAc	1.0	0.992
Water*	0.0	0.0
Column design:	$N_T = 48$, $f = 11$,	$r = 3.9$, $s = 9.5$

Figure 5b, we found a final design by doing repeated simulations. The results are in good agreement with the flash cascade prediction, as shown in Table 3. The composition profiles from the simulation are shown in Figure 6.

Note that we applied the lever rule to satisfy the overall mass balance in reaction invariant space for a reactive column operated in the kinetically controlled regime. Barbosa and Doherty (1988a,b) and Ung and Doherty (1995a) showed that the transformed lever rule is the necessary and sufficient condition for satisfying the overall mass balance for a column in the limit of chemical equilibrium. It is shown in Appendix A that the transformed lever rule is a necessary (but not sufficient) condition for satisfying overall mass balance for columns operated in the nonreactive and kinetically controlled regimes. However, it is still very helpful in quickly assessing feasibility of reactive distillation. Thus, we use the transformed lever rule to devise splits under a weaker condition of feasibility.

Algorithm for single – feed columns

We can estimate the direct and indirect split products for single–feed columns with the following general algorithm.

(a) Select column configuration:

(1) For a specified column pressure, plot the feasibility diagram. The feasibility diagram comprises the unstable node branches in the rectifying cascade (Eq. 4) and the stable node branches of the stripping cascade (Eqs. 3).

(2) From the feasibility diagram, select the column configuration for a single–feed column (reactive or hybrid) which provides the desired product, using the approach used in Figure 4. Also, select a D at which the reactive sections should be operated to get the desired product.

(3) If no single–feed column configuration (fully reactive or hybrid) provides the desired product, stop. Else, estimate a feasible split as provided below.

(b) Estimate feasible split:

(1) Solve the reactive stripping and rectifying cascade equations (Eqs. 1 and 2, respectively) at the D value selected in **part a** for a given feed composition until they reach their respective pinch points.

(2) If the column configuration selected in **part a** is fully reactive, go to step 3. Otherwise, depending on the hybrid column configuration selected in **part a**, solve Eqs. 1 and/or 2 again at $D = 0$ (no reaction limit) with the feed composition as the pinch point compositions of the respective reactive flash cascades obtained in step 1.

(3) Convert the iterates of the stripping cascade trajectories obtained in steps 1 and 2 to reaction invariant compositions (Ung and Doherty, 1995b) using Eq. 7. Similar expressions for the rectifying cascade trajectory are obtained in the reaction invariants for the vapor phase Y_i.

(4) Plot these projections of trajectories in reaction invariant space.

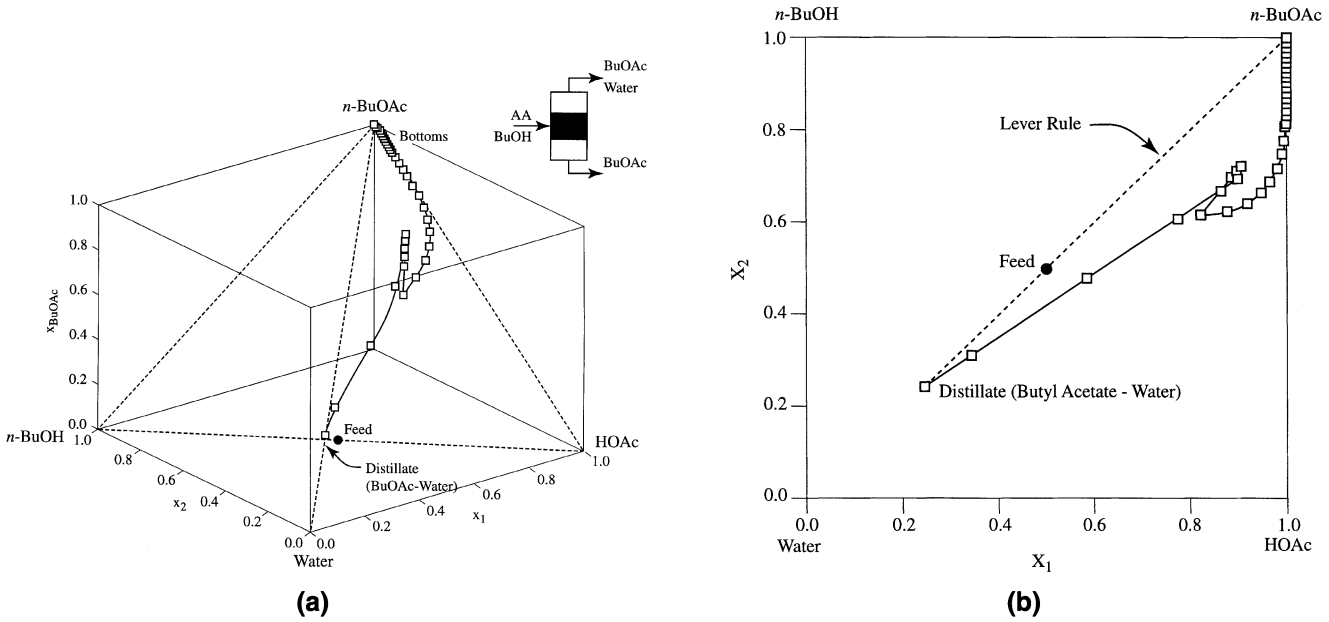

Figure 6. Column simulation profiles for a single-feed hybrid configuration for butyl acetate system in: (a) composite variable space; (b) reaction invariant space.

(5) Select the desired product composition as a potential product from a single–feed continuous column.

(6) Apply the transformed lever rule for continuous columns by which the bottoms, feed, and distillate compositions in reaction invariants must be collinear. Draw a straight line joining the desired product and the reaction invariant feed composition and extend it until it intersects the other cascade trajectory. The point of intersection indicates a feasible split. Convert the reaction invariant compositions back to mole fractions compositions.

Feasibility of Double–Feed Columns

It is not always possible to obtain the desired products from a single–feed column. For some systems, feeding the reactants together at the same stage does not provide good contacting. This is because the light boiling reactants move up the column and the high boiling reactants move down the column, thus, providing very little contact between them and resulting in low conversions. This problem can be circumvented if the lighter reactant is fed below the heavier reactant. It is helpful to know what feasible splits are possible for such a double–feed arrangement.

For example, consider the esterification of acetic acid with methanol at 1 atm

$$\text{Methanol(MeOH)} + \text{AceticAcid(HOAc)} \Leftrightarrow \text{MethylAcetate(MeOAc)} + \text{Water}(H_2O) \quad (9)$$

The rate expression is given by

$$r = k_f\left(a_{\text{HOAc}}a_{\text{MeOH}} - \frac{a_{\text{MeOAc}}a_{H_2O}}{K_{\text{eq}}}\right) \quad (10)$$

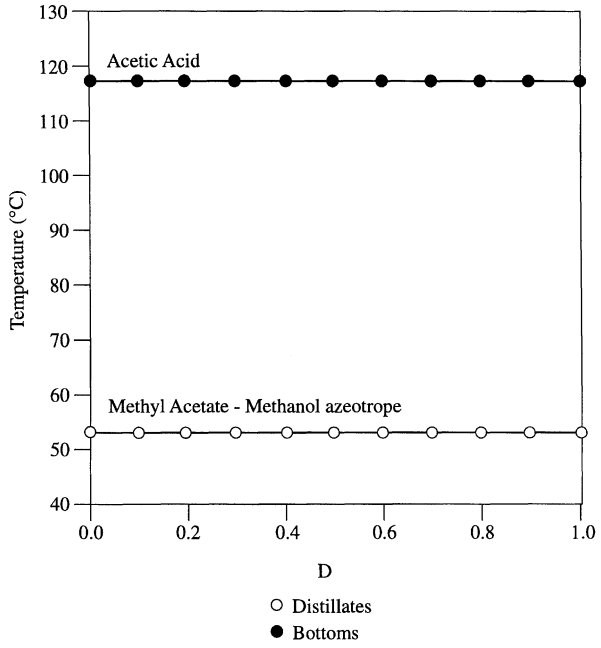

Figure 7. Feasibility diagram for methyl acetate at 1 atm.

where the expressions for k_f and K_{eq} depend on temperature and were taken from Huss et al. (1999). The vapor–liquid equilibrium was modeled with the Wilson equation in the liquid and the vapor was taken as ideal, except for dimerization of acetic acid. The binary interaction parameters were also taken from Huss et al. (1999).

A feasibility diagram for the methyl esterification example is shown in Figure 7. For any D, it is possible to obtain acetic acid as a potential bottoms product and a binary mixture of MeOAc and MeOH as potential distillate from a single–feed column. However, high purity MeOAc cannot be obtained at any D from a single–feed column, fully reactive or hybrid. The reason is because the two reactants, MeOH and HOAc have boiling points that are widely different (58°C and 117°C, respectively) and feeding them on the same stage leads to rapid separation, permitting little reaction between the two. On the other hand, for the BuOAc example, the boiling points of BuOH and HOAc are nearly the same (around 117°C); therefore, a single–feed column can be used to produce high purity BuOAc (Figures 4 and 5).

To study the feasibility of a double–feed column configuration, we use a countercurrent cascade shown in Figure 8. Saturated liquid and vapor reactant feeds are provided at the top and bottom, respectively. The product from the top of the cascade is vapor V and the product from the bottom of the cascade is liquid L. For simplicity, we consider a single chemical reaction with an equimolar chemistry and a heat of reaction negligible in comparison to the heat of vaporization of the mixture. (A more general cascade model is provided in Appendix B.) Under conditions of constant molar overflow (CMO), the liquid and vapor flows from stage to stage are equal and with n stages

$$V = V_1 = V_2 = \ldots = V_j = \ldots = V_{n+1} = F_L$$
$$F_U = L_0 = L_1 = \ldots = L_j = \ldots = L_n = L \quad (11)$$

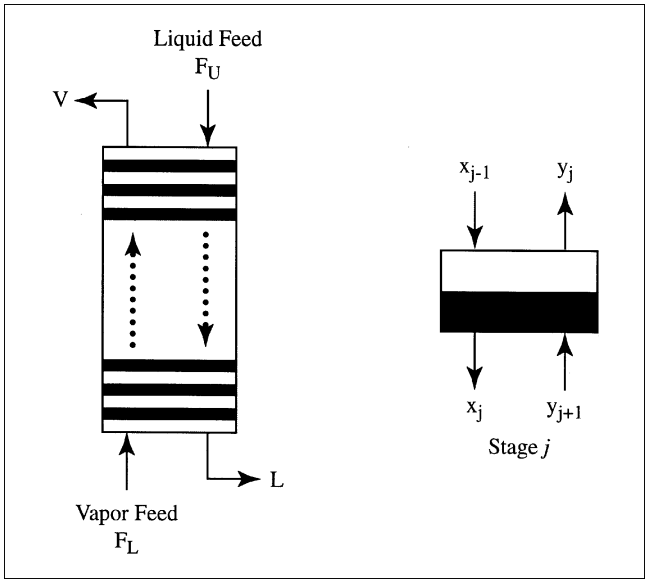

Figure 8. Countercurrent cascade and stage *j* of the cascade.

where F_L and F_U are the molar flow rates for the lower and upper feeds, respectively. A dynamic model for the jth stage of the countercurrent cascade is

$$H\left(\frac{dx_{i,j}}{dt}\right) = L(x_{i,j-1} - x_{i,j}) + V(y_{i,j+1} - y_{i,j}) + \nu_i k_f Hr(\boldsymbol{x}_j) \quad (i = 1...c-1) \quad (j = 1...n) \quad (12)$$

Two independent parameters characterize the countercurrent cascade:

(1) $F_r = F_L/F_U = V/L$, the molar feed ratio of the two feeds;

(2) $Da = (H/F_U)/(1/k_{f,\mathrm{ref}})$, the Damköhler number for the countercurrent cascade. This is the ratio of the characteristic liquid residence time to a characteristic reaction time. H is the liquid holdup on a stage and is assumed equal on all stages. $k_{f,\mathrm{ref}}$ is the forward rate constant at a reference temperature T_{ref}.

The model for the countercurrent cascade is

$$\left(\frac{dx_{i,j}}{\left(\frac{L}{H}dt\right)}\right) = (x_{i,j-1} - x_{i,j}) + F_r(y_{i,j+1} - y_{i,j}) + \nu_i Da\left(\frac{k_f}{k_{\mathrm{f,ref}}}\right) r(\boldsymbol{x}_j) \quad (i = 1...c-1) \quad (j = 1...n) \quad (13)$$

We introduce a dimensionless "warped" time $d\xi = Ldt/H$, and expressing the above equation in terms of $D = Da/(1 + Da)$, we get the model for countercurrent cascade

$$\left(\frac{dx_{i,j}}{d\xi}\right) = (x_{i,j-1} - x_{i,j}) + F_r(y_{i,j+1} - y_{i,j}) + \nu_i\left(\frac{k_f}{k_{f,\mathrm{ref}}}\right)\left(\frac{D}{1-D}\right) r(\boldsymbol{x}_j) \quad (i = 1...c-1) \quad (j = 1...n) \quad (14)$$

where $\boldsymbol{x}_0 = \boldsymbol{X}_{F,U}$ and $\boldsymbol{y}_{n+1} = \boldsymbol{y}_{F,L}$.

The entire countercurrent cascade is solved simultaneously as a set of $n(c-1)$ coupled ordinary differential equations for the two specified feed compositions $\boldsymbol{x}_{F,U}$, $\boldsymbol{y}_{F,L}$, and for specified values of the two parameters F_r and D. The simulation is continued until the liquid compositions on all stages reach their respective steady states. We have found that a dynamic model is more robust than a steady-state model, although more computationally demanding.

To demonstrate the method, we solve the reactive countercurrent cascade for the methyl esterification example introduced in Eq. 9. A saturated liquid acetic acid feed (heavy reactant) is provided at the top of the countercurrent cascade, and a saturated vapor methanol feed (light reactant) is provided at the bottom. For a given F_r and D, countercurrent cascade (Eq. 14) is solved for a large number of stages (typically 100) and for a sufficiently long time until the liquid compositions on all stages reach their steady states. The trajectory of liquid compositions at steady state is then plotted in the composite variable space which is 3-D for this example. The composite variables are x_{MeOAc} along with

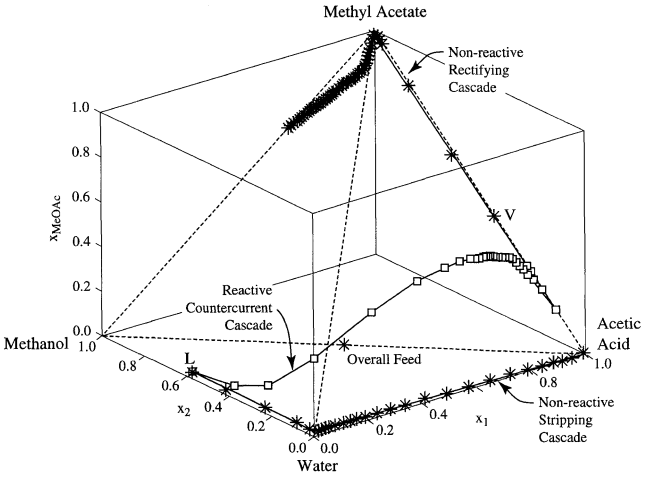

Figure 9. Flash cascade trajectories for a double-feed hybrid column for methyl acetate system in composite variable space.

$$X_1 = x_{\mathrm{HOAc}} + x_{\mathrm{MeOAc}}$$
$$X_2 = x_{\mathrm{MeOH}} + x_{\mathrm{MeOAc}} \quad (15)$$

Figure 9 shows the countercurrent cascade trajectory for $F_r = 1.0$ at $D = 0.8$. The trajectory of liquid compositions begins from near the MeOH–water edge (shown as L in Figure 9) and ends near the MeOAc-HOAc edge (shown as V in Figure 9). It exhibits a near pinch in the middle. A key feature of this cascade is that the compositions of the two products from the countercurrent cascade do not change after the pinch develops. Any increase in the number of stages after the pinch develops has no impact on the product compositions. (The fixed point criteria for the countercurrent cascade are provided in Appendix C.) The feature that makes the countercurrent cascade useful for this particular example is that the product compositions are close to the MeOH–water and MeOAc–HOAc edges, respectively. This property of the reactive countercurrent cascade trajectory to stretch from edge to edge makes double-feed columns an attractive proposition for producing desired products of pure MeOAc and pure water.

We can combine the reactive countercurrent cascade (Figure 8) with the rectifying and stripping cocurrent cascades (Figure 1) as a basis for estimating feasible products from a double-feed column. This arrangement is shown in Figure 10. The countercurrent cascade (Eq. 14) is solved for a large number of stages (n) at specified feed compositions, F_r, and D. The vapor product from the countercurrent cascade is input as feed to the cocurrent rectifying cascade (Eq. 2), which can either be reactive or nonreactive and is solved until a pinch point is reached. In a similar fashion, the liquid product from the bottom of the countercurrent cascade is sent as

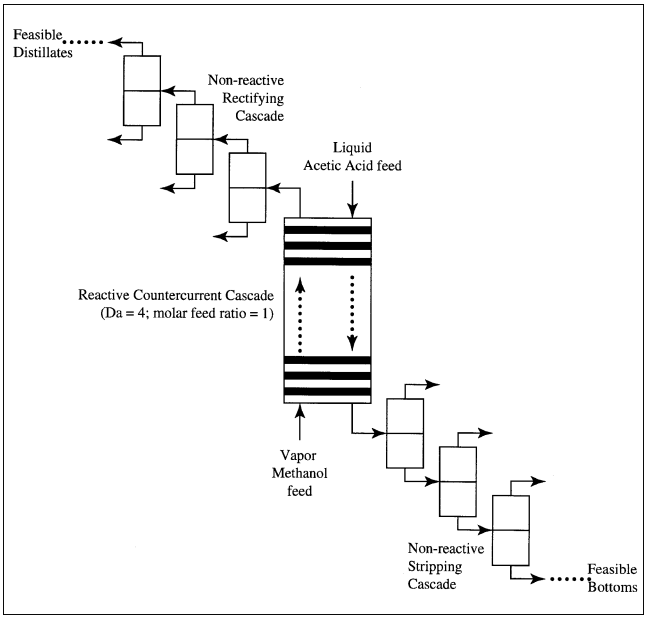

Figure 10. Flash cascade representation of a double-feed, hybrid column.

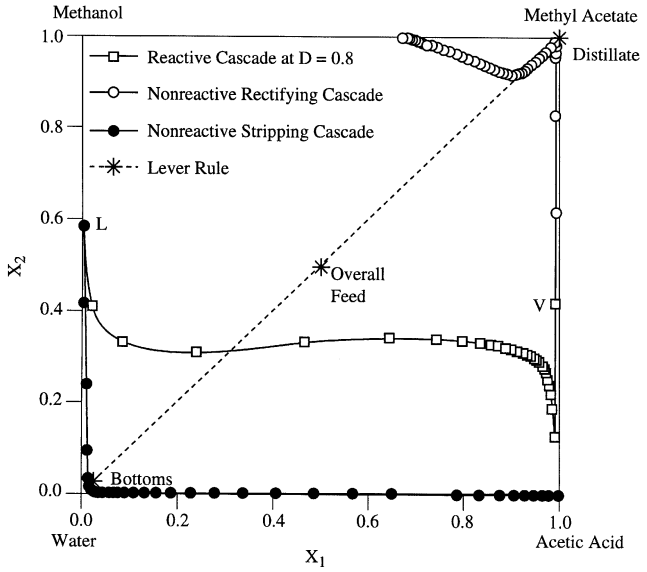

Figure 11. Flash cascade trajectories for a double-feed hybrid column for methyl acetate system in reaction invariant space at 1 atm.

feed to the cocurrent stripping cascade (Eq. 1), which can also be reactive or nonreactive as desired. This cascade is also solved until a pinch point is reached.

Figure 9 shows the cascade trajectories for the representation in Figure 10. The upper and lower feeds are pure acetic acid and methanol, respectively. The countercurrent cascade is reactive with $F_r = 1.0$ at $D = 0.8$. The cocurrent cascades are nonreactive. Note that the nonreactive rectifying trajectory starts near the MeOAc–HOAc edge (shown as V in Figure 9), remains close to that edge while moving up towards the MeOAc vertex, approaches the MeOAc vertex and then moves away, passing close to the MeOAc–water azeotrope before finally settling at its pinch point which is the MeOH–MeOAc azeotrope. On the other end, the nonreactive stripping trajectory starts close to the MeOH–water edge (shown as L in Figure 9), moves towards the water vertex, comes close to the water vertex, and then moves away, finally settling at a pinch point which is nearly pure acetic acid.

To select a feasible split for a double–feed column, the cascade trajectories in the composite variable space shown in Figure 9 are projected onto the reaction invariant space, as shown in Figure 11. We pick the iterate on the nonreactive rectifying cascade trajectory in Figure 11 that has the maximum MeOAc composition as distillate. Next, we draw a

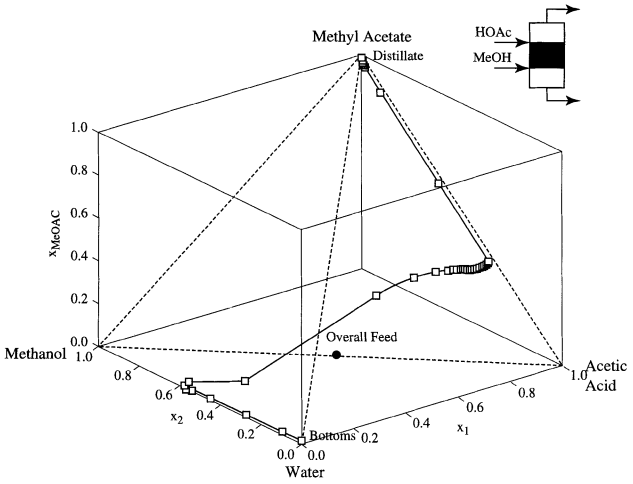

(a)

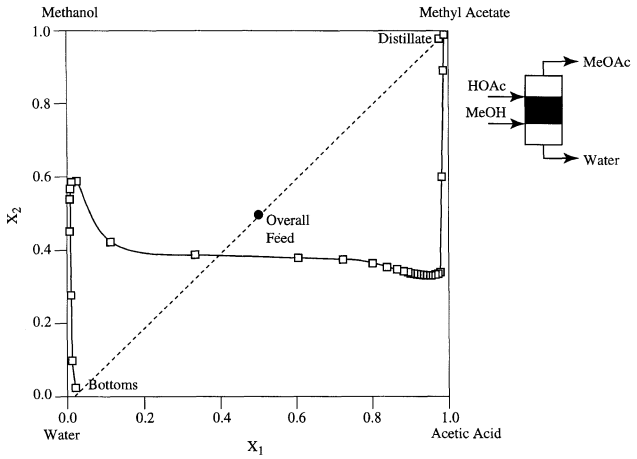

(b)

Figure 12. Column simulation profiles for a double-feed hybrid configuration for methyl acetate system in: (a) composite variable space; (b) reaction invariant space.

Table 4. Feasible Splits Predicted for Methyl Acetate by the Double–Feed Hybrid Model vs. Column Simulations at $D = 0.8$ for Splits in Figures 11 and 12

Mole Fraction	Cascade Prediction	Column Simulation*
Distillate		
HOAc	0.0	0.00001
MeOH	0.001	0.003
MeOAc	0.9792	0.975
Water	0.0198	0.02
Bottoms		
HOAc	0.025	0.025
MeOH	0.025	0.024
MeOAc	0.0	0.0
Water*	0.95	0.951
Column design:	$N_T = 36$, $f_u = 4$, $f_l = 28$,	$r = 1.3$, $s = 2.3$

straight lever rule mass balance line joining the distillate and the overall feed composition and extend it to intersect the nonreactive stripping cascade trajectory. The point of intersection is a feasible bottoms composition. The reaction invariant compositions are then converted back to mole fractions. The feasible split predictions for a double–feed hybrid column are provided in Table 4.

To verify that the estimate of the feasible split at $D = 0.8$ is achievable, we also simulated double–feed hybrid columns. The column simulation trajectories at $D = 0.8$ are shown in Figure 12. The composition of the products obtained and the column designs are provided in Table 4. The estimate of the feasible split from the double–feed cascade compares well with the results of full column simulations.

The double–feed column configuration developed here for methyl acetate synthesis is an alternative to the Eastman process (Agreda and Partin, 1984; Agreda et al., 1990). Figure 13 compares the two column configurations. The Eastman process is based on a homogeneous catalyst (sulfuric acid which is present throughout the bottom of the column, thereby preventing the use of a nonreactive stripping section), whereas the alternative design synthesized in this work is based on a heterogeneous catalyst which can be confined to specific parts of the column, therefore, allowing for a nonreactive stripping section. Another difference between the two designs is the absence of a distinct nonreactive extractive section in the design synthesized in this work. In the Eastman process config-

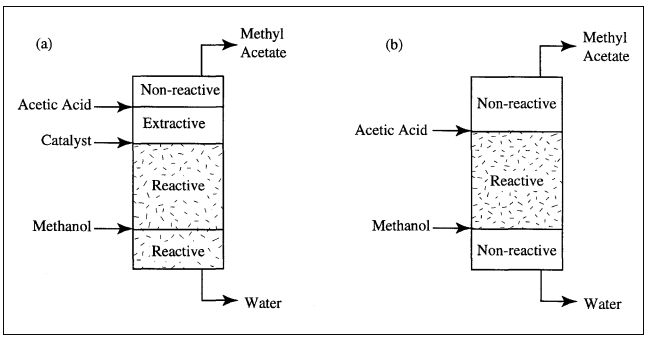

Figure 13. Column configurations for methyl acetate synthesis: (a) Eastman process; (b) this work.

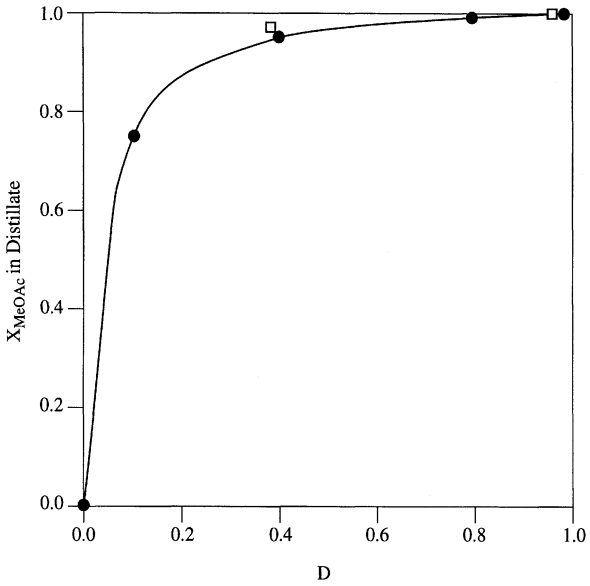

Figure 14. Product purity diagram for methyl acetate system.

Open squares are independent column designs by Huss et al. (1999).

uration, the methyl acetate–water azeotrope is obtained at the top of the reactive zone. This azeotrope is then broken by the addition of an extractive agent, acetic acid. Hence, the need for a nonreactive extractive section (Siirola, 1996). In the design alternative synthesized here, a distinct extractive section is not required. Figure 9 shows that it is the reaction zone alone between the two feeds that brings the products from this zone close to the MeOAc–HOAc and MeOH–water edges, respectively. Consequently, the separation at the two edges is very nearly like binary nonreactive separations resulting in high purity MeOAc and water products.

We used a constant value of $D = 0.8$ per stage in Figures 11 and 12. We do not know for what range of D, we can obtain MeOAc as a high–purity product from a double–feed column configuration. To determine this, we plot a *product purity diagram*. The countercurrent/cocurrent cascade model is solved at different D and the maximum desired product composition (MeOAc in this example) obtained from the hybrid cascade at each D is noted. A plot of the maximum MeOAc composition in the distillate vs. D is shown in the product purity plot in Figure 14. From this plot, it can be seen that, for $D \geq 0.4$ in the double–feed hybrid column, the MeOAc composition is greater than 95%. Therefore, we could choose a $D \geq 0.4$ in the column to obtain fairly pure MeOAc. Results of independent simulations of double–feed hybrid columns by Huss et al. (1999) are in good agreement with this estimate.

Effect of pressure on feasibility

Column pressure has an effect on the purity of the desired product. Intuitively, it may seem that an increase in pressure increases reaction rates due to higher temperatures so that higher reactant conversions should be possible. If this is cor-

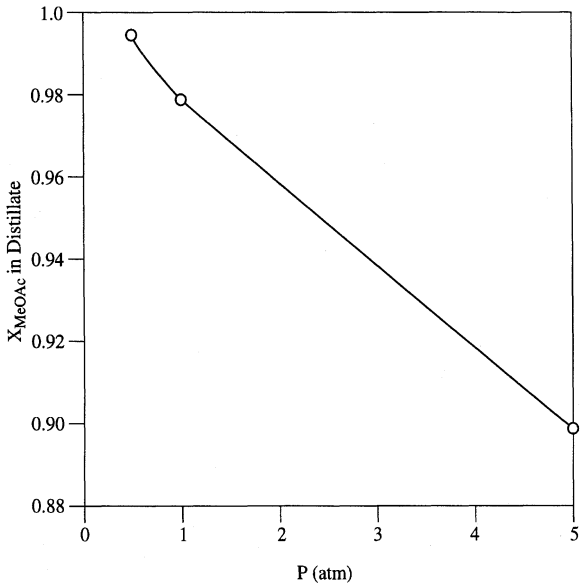

Figure 15. Pressure effect on feasibility of a double-feed hybrid column for methyl acetate synthesis.

rect, then increasing the column pressure should also lead to an increase in the product purities for the MeOAc system. In fact, the reverse happens! For example, Agreda and Partin (1984) reported that higher purities of methyl acetate are obtained at lower pressures for the Eastman process. Figure 15 shows the effect of pressure on the maximum MeOAc composition in the distillate. Each of the data points were calculated for the arrangement shown in Figure 10 with $D = 0.8$/stage, $F_r = 1$ for the countercurrent reactive cascade, and $D = 0$ for the cocurrent cascades.

It can be seen that lowering the pressure leads to higher MeOAc purity. This is caused by the interaction of pressure and temperature with the VLE, as reflected in the location of pinches in the countercurrent cascade and, consequently, in the reactive middle section of the column. Figure 16 shows the trajectories corresponding to 0.5 and 5 atm, respectively. At 0.5 atm, the pinch in the countercurrent cascade is closer to the MeOAc–HOAc edge and, hence, the vapor product from the top of the countercurrent cascade lies very close to the edge. This leads to an easier separation in the nonreactive cocurrent cascade above the reactive cascade, with the cocurrent cascade trajectory reaching close to the MeOAc edge. At 5 atm, the pinch in the countercurrent cascade is far from the MeOAc–HOAc edge, and, consequently, the vapor product also lies farther from the edge. This causes the trajectory of the nonreactive cocurrent cascade to be far from the MeOAc edge and, hence, leads to a split with lower purity of methyl acetate. Independent column simulations at different pressures provide splits that are in agreement with those in Figure 16 (Tio, 2000).

Isopropyl Acetate Synthesis

In this section we combine the tools developed in the previous sections to assess the feasibility of various column configurations. This approach is illustrated on isopropyl acetate synthesis.

Consider the esterification of acetic acid with isopropanol at a pressure of 1 atm.

$$\text{Isopropanol(IPA)} + \text{Acetic Acid(HOAc)} \Leftrightarrow \text{Isopropyl Acetate(IPOAc)} + \text{water}(H_2O) \quad (16)$$

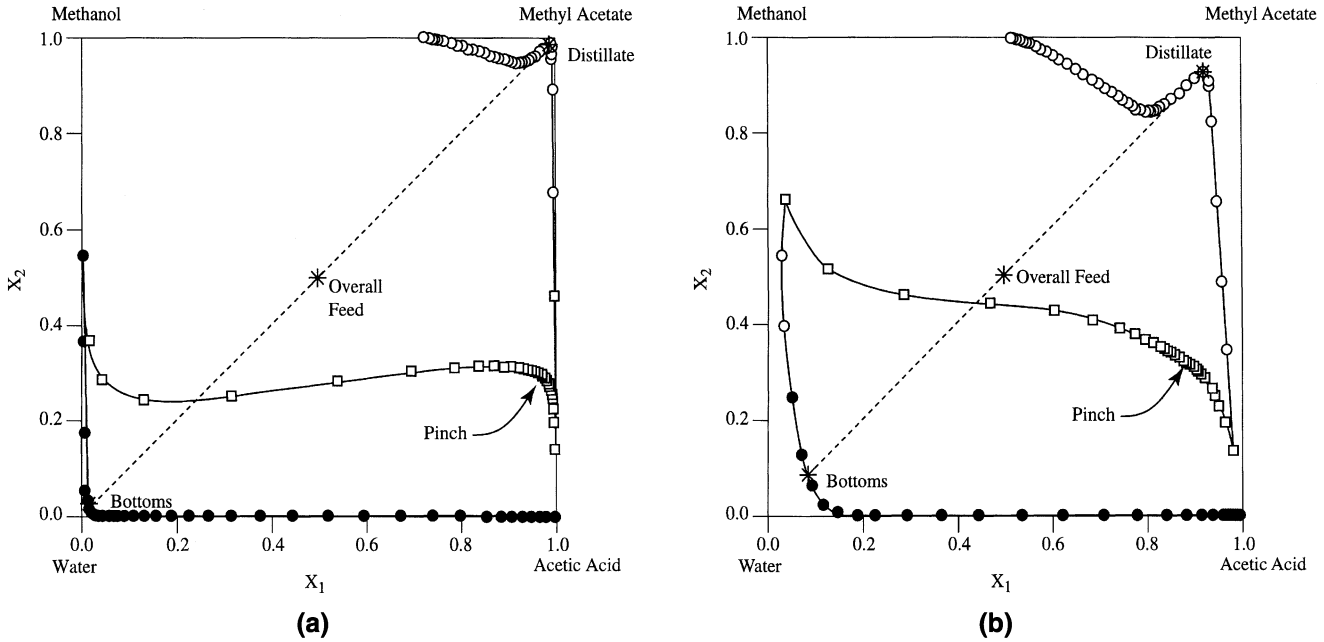

Figure 16. Flash cascade trajectories for a double-feed hybrid column for methyl acetate system in reaction invariant space: (a) at 0.5 atm; (b) at 5 atm.

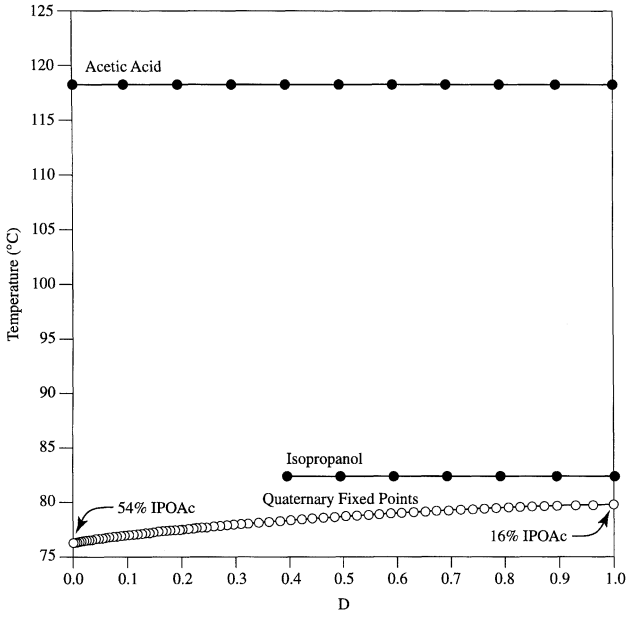

Figure 17. Feasbility diagram for isopropyl acetate system at 1 atm.

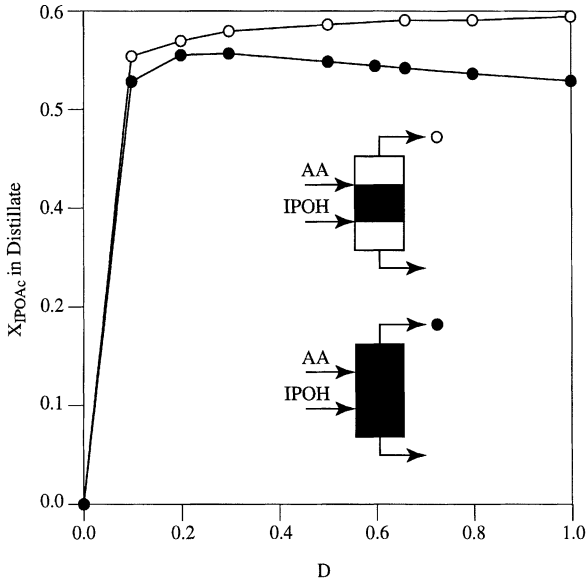

Figure 18. Product purity diagram for isopropyl acetate system.

We represent the kinetics by a homogeneous model

$$r = k_f \left(a_{\mathrm{HOAc}} a_{\mathrm{IPA}} - \frac{a_{\mathrm{IPOAc}} a_{\mathrm{H_2O}}}{K_{\mathrm{eq}}} \right) \tag{17}$$

where k is taken as constant over the temperature range of interest, so that $k_f/(k_{f,\mathrm{ref}}) = 1$.

The reaction equilibrium constant has a constant value of approximately 8.7 in the temperature range of interest (Lee and Kuo, 1996). The vapor-liquid equilibrium was modeled using the Antoine vapor pressure equation and the NRTL equation for activity coefficients in the liquid phase; the vapor phase was taken as ideal, except for dimerization of the acetic acid. The physical property information was taken Venimadhavan et al. (1999b, Table 3).

We seek to answer two questions. Is it possible to obtain isopropyl acetate from a simple, two–product column? If so, what column configuration and rate of reaction will provide the desired product?

We first calculate the feasibility diagram for a single–feed column, shown in Figure 17. Pure isopropyl acetate cannot be obtained as a product from any single–feed column; reactive or hybrid. Isopropyl acetate can only be obtained as part of a quaternary mixture as distillate with the purity of isopropyl acetate varying from 54% at $D = 0$ to 16% at $D = 1$.

The product purity diagram for a double–feed hybrid column (reactive middle section and nonreactive rectifying and stripping sections with the upper feed of acetic acid and lower feed of isopropanol and $F_r = 1$) and a double–feed reactive column are shown in Figure 18. The diagram shows that pure isopropyl acetate cannot be obtained from a double–feed column either. The best possible split with the configurations considered here contains 58% isopropyl acetate in a ternary mixture with isopropanol and water. This is obtained from a double–feed hybrid column with a reactive middle section and nonreactive rectifying and stripping sections for $D \geq 0.4$.

Therefore, for this example, we can quickly conclude that pure isopropyl acetate cannot be obtained by reactive distillation in any of the hybrid or fully-reactive column configurations considered.

Summary and Conclusions

This article describes a systematic method for synthesizing feasible column designs for reactive distillation. The method requires three basic building blocks for synthesizing different hybrid column configurations. These are

(a) A cocurrent rectifying cascade
(b) A cocurrent stripping cascade
(c) A countercurrent cascade.

These building blocks may be reactive or nonreactive as desired. Mixing and matching these blocks leads to various column configurations. The different column configurations that can be potentially evaluated with the help of only these building blocks are: (1) single–feed or double–feed columns; and (2) fully reactive or hybrid columns.

We have developed tools that can be used to quickly screen the different hybrid column configurations and decide at a very early design stage if there is an incentive in investing more time and resources in the further study of a process alternative.

These methods were illustrated on three esterification examples, each with a single reaction (the approach can also be applied to cases with more reactions and components; see Chadda, 2001). In spite of the fact that the examples form a homologous series, the feasible designs are quite different. While a single–feed hybrid column was sufficient to provide butyl acetate, a double–feed column was required to produce high purity methyl acetate. In the case of isopropyl acetate system no reactive column configurations considered

were suitable for the production of high purity isopropyl acetate.

Finally, we would like to point out some limitations of the approach and examples.

(1) Using these building blocks in different permutations can lead to a very large number of hybrid column configurations. In this article we have dealt with only a small number of these configurations. However, the methods outlined here can be used as a basis for generating a computer-aided method for synthesizing more configurations, such as complex columns, and evaluating their feasibility.

(2) The value of *Da* is taken as a constant within the reactive sections. This is certainly not necessary, and parametric studies may reveal additional feasible splits.

(3) There are many other parameters such as feed ratio, type and location of multiple feeds and side draws, reflux and reboil ratios, and the choice of joining the building blocks of cascades at or near pinch compositions. These variables can also be studied parametrically, for which an optimization approach may be effective.

(4) We have not studied examples with many more degrees of freedom, or with significant heats of reaction.

Acknowledgments

We are grateful for support from sponsors of the Process Design and Control Center at the University of Massachusetts, Amherst and from the National Science Foundation (grant number CTS-9613489).

Notation

a_i = activity of i
c = total number of components
D = scaled Damköhler number, $= Da/\{1 + Da\}$, dimensionless
Da = Damköhler number, dimensionless
f_r = feed stage location in a continuous distillation column
F_r = ratio of the molar feed rates in a countercurrent cascade
F_L = molar feed flow rate for the lower feed, mol/h
F_U = molar feed flow rate for the upper feed, mol/h
H = liquid holdup on a stage, mol
k_f = forward reaction rate constant, moles reacted per mole of mixture per unit time
$k_{f,\mathrm{ref}}$ = forward reaction rate constant at the reference temperature, mole reacted per mole of mixture per unit time
K_{eq} = reaction equilibrium constant
L = liquid flow rate, mol/time
P = system pressure, atm
$M(\boldsymbol{x})$ = average molecular weight $(= \sum_{i=1}^{C} M_i x_i)$
M = index for cocurrent rectifying cascade
n = index for countercurrent reactive cascade
N = index for cocurrent stripping cascade
N_T = number of equilibrium stages in a continuous distillation column
$r(\boldsymbol{x})$ = driving force for the reaction, $(\prod_{\mathrm{reactants}} a_i^{-\nu_i} - \pi_{\mathrm{products}} \times a_i^{\nu_i}/K_{\mathrm{eq}})$
r = reflux ratio
s = reboil ratio
T = temperature
V = vapor flow rate, mol/time
$\boldsymbol{x}$ = state vector of liquid phase mole fractions
x_i = mole fraction of i in the liquid phase
X_i = reaction invariant in the liquid phase
y_i = mole fraction of i in the vapor phase
Y_i = reaction invariant in the vapor phase

Greek letters

γ_i = liquid activity coefficient
ν_i = stoichiometric coefficient for i
ν_T = summation of all stoichiometric coefficients
ϕ_j = fraction of feed vaporized in j^{th} flash unit

Subscripts and superscripts

0 = initial condition
B = bottoms
D = distillate
F = feed
i = component index
j = stage index for flash cascade
ref = reference
L = lower
O = overall
U = upper
$\wedge$ = pinch composition

Literature Cited

Agreda, V. H., L. R. Partin, and W. H. Heise, "High–Purity Methyl Acetate via Reactive Distillation," *Chem. Eng. Prog.*, **86**, 40 (1990).
Agreda, V. H., and L. R. Partin, "Reactive Distillation Process for Production of Methyl Acetate," U.S. Patent No. 4,435,595 (1984).
Backhaus, A. A., "Continuous Process for Manufacture of Esters," U.S. Patent No. 1,400,849 (1921).
Barbosa, D., and M. F. Doherty, "Design and Minimum Reflux Calculations for Single-Feed Multicomponent Reactive Distillation Columns," *Chem. Eng. Sci.*, **43**, 1523 (1988a).
Barbosa, D., and M. F. Doherty, "Design and Minimum Reflux Calculations for Double-Feed Multicomponent Reactive Distillation Columns," *Chem. Eng. Sci.* **43**, 2377 (1988b).
Bessling, B., G. Schembecker, and K. H. Simmrock, "Design of Processes with Reactive Distillation Line Diagrams," *Ind. Eng. Chem. Res.*, **36**, 3032 (1997).
Buzad, G., and M. F. Doherty, "Design of Three-Component Kinetically Controlled Reactive Distillation Columns Using Fixed-Point Methods," *Chem. Eng. Sci.*, **49**, 1947 (1994).
Cardoso, M. F., R. L. Salcedo, S. Feyo de Azevedo, and D. Barbosa, "Optimization of Reactive Distillation Processes with Simulated Annealing," *Chem. Eng. Sci.*, **55**, 5059 (2000).
Chadda, N., M. F. Malone, and M. F. Doherty, "Feasible Products for Kinetically Controlled Reactive Distillation of Ternary Mixtures," **46**, 923 (2000).
Chadda, N., M. F. Malone and M. F. Doherty, "Effect of Chemical Kinetics on Feasible Splits for Kinetically Controlled Reactive Distillation," *AIChE J.*, **47**, 590 (2001).
Chadda, N., "Feasibility of Kinetically Controlled Reactive Distillation," PhD Diss., University of Massachusetts, Amherst (2001).
Ciric, A. R., and D. Gu, "Synthesis of Nonreactive Reactive Distillation Processes by MINLP Optimization," *AIChE J.*, **40**, 1479 (1994).
Damköhler, G., "Stromungs und warmeubergangsprobleme in chemischer technik and forschung," *Chem. Ing. Tech*, **12**, 469 (1939).
Espinosa, J., P. A. Aguirre, and G. A. Perez, "Product Composition Regions of Single-Feed Reactive Distillation Columns: Mixtures Containing Inerts," *Ind. Eng. Chem. Res.*, **34**, 853 (1995).
Fidkowski, Z. T., M. F. Doherty, and M. F. Malone, "Feasibility of Separations for Distillation of Nonideal Ternary Mixtures," *AIChE J.*, **39**, 1303 (1993).
Giessler, S., R. Y. Danilov, R. Y. Pisarenko, L. A. Serafimov, S. Hasebe, and I. Hashimoto, "Feasibility Study of Reactive Distillation using the Analysis of the Statics," *Ind. Eng. Chem. Res.*, **37**, 4375 (1998).
Giessler, S., R. Y. Danilov, R. Y. Pisarenko, L. A. Serafimov, S. Hasebe, and I. Hashimoto, "Feasibility Separation Modes for Various Reactive Distillation Systems," *Ind. Eng. Chem. Res.*, **38**, 4060 (1999).
Hauan, S., K. M. Lien, and A. W. Westerberg, "Phenomena-Based Analysis of Fixed Points in Reactive Separation Systems," *Chem. Eng. Sci.*, **55**, 1053 (2000).
Huss, R. S., F. Chen, M. F. Malone, and M. F. Doherty, "Computer-Aided Tools for the Design of Reactive Distillation Systems," *Comput. Chem. Eng.*, S955 (1999).
Ismail, S. R., E. N. Pistikopoulos, and K. P. Papalexandri, "Synthesis of Reactive and Combined Reactor/Separation Systems Utilizing a

Mass/Heat Exchange Transfer Module," *Chem. Eng. Sci.*, **54**, 2721 (1999).
Keyes, D. B., "Esterification Processes and Equipment," *Ind. Eng. Chem.*, **24**, 1096 (1932).
Lee, J. W., S. Hauan, and A. W. Westerberg, "Circumventing an Azeotrope in Reactive Distillation," *Ind. Eng. Chem. Res.*, **39**, 1061 (2000a).
Lee, J. W., S. Hauan, and A. W. Westerberg, "Graphical Methods for Reactive Distribution in a Reactive Distillation Column," *AIChE J.*, **46**, 1218 (2000b).
Lee, L.-S., and M.-Z. Kuo, "Phase and Reaction Equilibria of the Isopropanol-Acetic Acid-Isopropyl Acetate Water System at 760 mm Hg.," *Fluid Phase Equilib.*, **123**, 147 (1996).
Longtin, B., and M. Randall, "Simultaneous Chemical Reaction and Fractional Distillation," *Ind. Eng. Chem.*, **34**, 292 (1942).
Melles, S., J. Grievink, and S. M. Schrans, "Optimization of the Conceptual Design of Reactive Distillation Columns," *Chem. Eng. Sci.*, **55**, 2089 (2000).
Okasinski, M. J., and M. F. Doherty, "Design Method for Kinetically Controlled, Staged Reactive Distillation Columns," *Ind. Eng. Chem. Res.*, **37**, 2821 (1998).
Papalexandri, K. P., and E. N. Pistikopoulos, "Generalized Modular Representation for Process Synthesis," *AIChE J.*, **42**, 1010 (1996).
Rooks, R. E., V. Julka, M. F. Doherty, and M. F. Malone, "Structure of Distillation Regions for Multicomponent Azeotropic Mixtures," *AIChE J.*, **44**, 1382 (1998).
Siirola, J. J., "Industrial Applications of Chemical Process Synthesis," *Adv. Chem. Eng.*, **23**, 1-62 (1996).
Tio, Guat-Lee, "Effect of Pressure on Kinetics and Selectivity of Methyl Acetate Synthesis," MS Thesis, University of Massachusetts, Amherst (2000).
Ung, S., and M. F. Doherty, "Synthesis of Reactive Distillation Systems with Multiple Equilibrium Chemical Reactions," *Ind. Eng. Chem. Res.*, **34**, 2555 (1995a).
Ung, S., and M. F. Doherty, "Vapor Liquid Phase Equilibrium in Systems with Multiple Chemical Reactions," *Chem. Eng. Sci.*, **50**, 23 (1995b).
Venimadhavan, G., M. F. Malone, and M. F. Doherty, "A Novel Distillate Policy for Batch Reactive Distillation with Application to the Production of Butyl Acetate," **38**, 714 (1999a).
Venimadhavan, G., M. F. Malone, and M. F. Doherty, "Bifurcation Study of Kinetic Effects in Reactive Distillation," *AIChE J.*, **45**, 546 (1999b).
Wahnschafft, O. M., J. W. Koehler, E. Blass, and A. W. Westerberg, "The Product Composition Regions of Single-Feed Azeotropic Distillation Columns," *Ind. Eng. Chem. Res.*, **31**, 2345 (1992).

Appendix A

Lever rule for hybrid columns

Consider a single–feed hybrid column with a molar feed flow rate F of composition x_F, a distillate flow rate D of composition x_D, and a bottoms flow rate B of composition x_B. Assume that a single chemical reaction $V + W = Y + Z$ takes place only on the reactive stages of the hybrid column. The material balance for the hybrid column is

$$Fx_{F,i} = Dx_{D,i} + Bx_{B,i} - \nu_i \epsilon \quad (i = 1, 4) \tag{A1}$$

where ϵ is the total extent of reaction in the column.

For a four component mixture with a single chemical reaction, we need one reference component. Thus, Eq. A1 can be written as three separate equations as follows

$$Fx_{F,\mathrm{ref}} = Dx_{D,\mathrm{ref}} + Bx_{B,\mathrm{ref}} + \nu_{\mathrm{ref}} \epsilon \tag{A2}$$

$$F = D + B \tag{A3}$$

$$Fx_{F,i} = Dx_{D,i} + Bx_{B,i} - \nu_i \epsilon \quad (i = 1,2) \tag{A4}$$

where the reference component is Y.

Using Eq. A2 to eliminate ϵ from Eq. A3 and Eq. A4 and rearranging, we get

$$Fx_{F,\mathrm{ref}} = Dx_{D,\mathrm{ref}} + Bx_{B,\mathrm{ref}} - \nu_{\mathrm{ref}} \epsilon \tag{A5}$$

$$F = D + B \tag{A6}$$

$$F\left(x_{F,i} - \nu_i \nu_{\mathrm{ref}}^{-1} x_{F,\mathrm{ref}}\right) = D\left(x_{D,i} - \nu_i \nu_{\mathrm{ref}}^{-1} x_{D,\mathrm{ref}}\right) + B\left(x_{B,i} - \nu_i \nu_{\mathrm{ref}}^{-1} x_{B,\mathrm{ref}}\right) \tag{A7}$$

where $i = 1,2$.

Equation A7 can be written in terms of reaction invariants as

$$FX_{F,i} = DX_{D,i} + BX_{B,i} \quad (i = 1, 2) \tag{A8}$$

where $X_{F,i} = (x_{F,i} - \nu_i \nu_{\mathrm{ref}}^{-1} x_{F,\mathrm{ref}})$, as given by Ung and Doherty (1995a). Equations A5, A6, and A7 represent the overall mass balance for a hybrid column.

Eliminating F from Eqs. A5 and A8 with the help of Eq. A6, we get three independent equations for representing the overall mass balance

$$\left(\frac{D}{B}\right) = \left(\frac{X_{F,i} - X_{B,i}}{X_{D,i} - X_{F,i}}\right) \quad (i = 1, 2) \tag{A9}$$

and

$$D(x_{F,\mathrm{ref}} - x_{D,\mathrm{ref}}) + B(x_{F,\mathrm{ref}} - x_{B,\mathrm{ref}}) + \nu_{\mathrm{ref}} \epsilon = 0 \tag{A10}$$

The necessary condition for satisfying the overall mass balance in a hybrid column is Eq. A9 whether the reaction is chemical equilibrium limited or not. This is also the sufficient condition when the reaction is chemical equilibrium limited as shown in Ung and Doherty (1995a). However, for kinetically controlled columns, the necessary and sufficient conditions for satisfying the overall mass balance in a hybrid column are given by Eqs. A9 and A10.

Appendix B

General two – feed flash cascade model

The model for the two–feed flash cascade model developed in this article is applicable to equimolar chemistries. However, if the chemistry is nonequimolar, it is advantageous to use parameters defined in terms of mass rather than moles. The reason is that, with mass based parameters, we can define a vapor mass fraction ϕ_m, and a feed ratio $F_{r,m}$ which are not functions of conversion. The resulting equations are as follows

Countercurrent Cascade (n Stages)

$$\left(\frac{dx_{i,j}}{d\xi}\right) = (x_{i,j-1} - x_{i,j}) + F_{r,m}\frac{M(\boldsymbol{x}_{j-1})}{M(\boldsymbol{y}_{j+1})}(y_{i,j+1} - x_{i,j}) + F_{r,m}\frac{M(\boldsymbol{x}_{j-1})}{M(\boldsymbol{y}_j)}(x_{i,j} - y_{i,j})$$

$$+(\nu_i-\nu_T x_i)\left(\frac{k_f}{k_{f,\mathrm{ref}}}\right)\frac{M(\boldsymbol{x}_{j-1})}{M(\boldsymbol{x}_j)}\left(\frac{D}{1-D}\right)r(\boldsymbol{x}_j)$$

$$(i=1\ldots c-1)$$

$$(j=1\ldots n) \quad \text{(B1)}$$

where $\boldsymbol{x}_0=\boldsymbol{x}_{F,U}$ and $\boldsymbol{y}_{n+1}=\boldsymbol{y}_{F,L}$

Rectifying Cocurrent Cascade (M Stages)

$$(x_{i,j}-y_{i,j-1})=\phi_m\frac{M(\boldsymbol{y}_{j-1})}{M(\boldsymbol{y}_j)}(x_{i,j}-y_{i,j})$$

$$+(\nu_i-\nu_T x_{i,j})\left(\frac{k_f}{k_{f,\mathrm{ref}}}\right)\left(\frac{D}{1-D}\right)\frac{M(\boldsymbol{y}_{j-1})}{M(\boldsymbol{x}_j)}r(\boldsymbol{x}_j)$$

$$(i=1\ldots c-1)$$

$$(j=1,2\ldots M) \quad \text{(B2)}$$

Stripping Cocurrent Cascade (N Stages)

$$(x_{i,j}-x_{i,j-1})=\phi_m\frac{M(\boldsymbol{x}_{j-1})}{M(\boldsymbol{y}_j)}(x_{i,j}-y_{i,j})$$

$$+(\nu_i-\nu_T x_{i,j})\left(\frac{k_f}{k_{f,\mathrm{ref}}}\right)\left(\frac{D}{1-D}\right)\frac{M(\boldsymbol{x}_{j-1})}{M(\boldsymbol{x}_j)}r(\boldsymbol{x}_j)$$

$$(i=1\ldots c-1)$$

$$(j=1,2\ldots N) \quad \text{(B3)}$$

It should be noted here that the dimensionless quantities D, $F_{r,m}$, and ϕ_m in these equations are defined with respect to mass flows and mass holdups. In the above equations, a new quantity $M(\boldsymbol{x})$ is introduced which is the average molecular weight, and appears as a consequence of using mass variables

$$M(\boldsymbol{x})=\sum_{i=1}^{c}M_i x_i \quad \text{(B4)}$$

Similar definitions apply to $M(\boldsymbol{y})$. Equations B1, B2, and B3 reduce to Eqs. 14, 2 and 1, respectively, when $\nu_T=0$.

Appendix C

Pinch point criteria for countercurrent cascade

At a steady state, the countercurrent cascade model (Eq. 14) is given by

$$(x_{i,j-1}-x_{i,j})+F_r(y_{i,j+1}-y_{i,j})$$

$$+\nu_i\left(\frac{k_f}{k_{f,\mathrm{ref}}}\right)\left(\frac{D}{1-D}\right)r(\boldsymbol{x}_j)=0$$

$$(i=1\ldots c-1)$$

$$(j=1\ldots n) \quad \text{(C1)}$$

The pinch point criterion for the countercurrent cascade (Eq. C1) is obtained when $(x_{i,j-1}-x_{i,j})=0$ as $n\to\infty$

$$r(\hat{\boldsymbol{x}})=0 \quad \text{(C2)}$$

Equation C2 implies that pinch points lie on the reaction equilibrium surface. However, Eq. C2 is just a necessary condition; the sufficient condition for the pinch point of the countercurrent cascade can be written in terms of reaction invariants by writing Eq. C1 for component i and a reference component k at the pinch composition $\hat{x}_i$ and adding the two. Thus, we get

$$(X_{0,i}-F_r Y_{1,i})=\left(\hat{X}_i-F_r\hat{Y}_i\right)=(X_{n,i}-F_r Y_{n+1,i})$$

$$(i=1\ldots c-2) \quad \text{(C3)}$$

Equations C2 and C3 can be used to determine the pinch point of the countercurrent cascade. The composition of the pinch point is independent of Da, but is dependent on the transformed feed compositions, $X_{0,i}$ and $Y_{n+1,i}$ and also the feed ratio F_r.

It has been shown in this article that the pinch points in a countercurrent cascade are located in the middle of the cascade (Figures 11 and 12). The reason for this is that the pinch points are constrained by an overall mass balance and the feed specification at the two ends of the cascade.

Manuscript received Dec. 12, 2001, and revision received July 17, 2002.